Revisiting Bandwidth of D-Band Patch and Stacked Patch Antennas Using Modal Analysis

Cao, Yuyan; Lau, Buon Kiong

Published in:
20th European Conference on Antennas and Propagation (EuCAP 2026)

DOI:
10.23919/EuCAP68105.2026.11611945

2026

Document Version:
Publisher's PDF, also known as Version of record

Revisiting Bandwidth of D-band Patch and Stacked Patch Antennas Using Modal Analysis

Yuyan Cao and Buon Kiong Lau
Department of Electrical and Information Technology, Lund University, Sweden, yu-yan.cao@eit.lth.se

***Abstract*—A rectangular conducting patch can be configured as a wideband or narrowband antenna, depending on its placement on the ground plane. The feeding method and the presence of a stacked patch also significantly influence the impedance bandwidth. In this context, the paper revisits the operating principles of patch antennas from the perspective of characteristic mode analysis (CMA), with a focus on implementing the antenna on low-cost substrate in the D-band. The results show that the fundamental mode's bandwidth increases dramatically with the height of the substrate. Practical feeding with a microstrip line severely degrades the modal bandwidth but also introduces a new broadside mode. Adding a stacked patch enhances both modes' bandwidths and enables joint excitation to achieve wideband dual-resonances, as demonstrated using a practical antenna design in full-wave simulation. Hence, CMA yields intuitive insight into the operation of patch and stacked patch antennas.**

***Index Terms*—Patch antenna, stacked patch, wideband antenna, characteristic mode analysis.**

I. Introduction

The D band (110-170 GHz) is a promising candidate for 6G wireless communication systems due to the availability of large absolute bandwidth (i.e., tens of GHz) to support extremely high data rates [1]. Establishing reliable links at these frequencies requires antennas that offer both wide impedance bandwidth and high gain, the latter due to the very high path loss. However, stringent fabrication tolerances and the cost/complexity of advanced antenna technologies make D-band antenna design challenging. Therefore, efforts have been made to apply low-cost multilayer High Density Interconnect (HDI) printed circuit board (PCB) technology for D-band antenna implementation [2].

Microstrip patch antennas are widely favoured for their low profile, low manufacturing cost, and ease of integration, but classical single-layer implementations are bandwidth-limited [3]–[5]. Several wideband techniques, such as the addition of U-slot [6], coupled-fed [7], and stacked patch structures [8], have been explored to overcome this constraint. Among them, the stacked configuration is popular, as it enables multiple resonances and delivers a more stable radiation pattern across a broad frequency range [8]. However, existing studies largely rely on parameter tuning and offer limited physical insight into the mechanisms behind bandwidth improvement.

Characteristic mode analysis (CMA) provides a systematic approach to reveal the modal behaviour and radiation mechanisms of antennas, offering valuable insight into how structural features affect radiation performance [9]. Moreover, the influence of the feed on the modal properties can also be studied when the feed position and configuration are chosen [10]. To date, numerous CMA-based studies have primarily concentrated on evolving single-layer microstrip antenna designs to improve performance. Common approaches include shaping slots on the patch to enhance bandwidth [11], [12], and modifying the placement of same-layer parasitic elements or adjusting the feed type and position to achieve circular polarisation [13], [14].

In this work, CMA is employed to revisit the fundamental operation of microstrip antennas implemented on low-cost HDI PCB substrates for D-band applications. The analysis focuses on the bandwidth characteristics of single-layer configurations and examines the impact of feed structure, dielectric loading, and stacked topology. Building on the insights gained, a stacked patch antenna is subsequently designed and verified through full-wave simulations, demonstrating a wideband dual-resonance response. Although the work is based on D-band, the findings are equally applicable to patch and stacked patch antennas operating in other frequency bands.

II. Characteristic Mode Analysis

A. Classical Theory of Conventional Patch Antenna

Conventional microstrip patch antennas are implemented on the top of a thin dielectric substrate, where the thickness h is small compared to the free-space wavelength λ_0, typically $0.003\lambda_0 < h < 0.05\lambda_0$ [15]. Patch dimensions are commonly chosen to support the fundamental TM_{10} mode. Together with the ground plane, the patch forms a resonant cavity, with the edges approximated as open-circuit walls. Consequently, most of the electromagnetic energy is confined within the cavity, yielding a high radiation quality factor Q_{rad}. Since the impedance bandwidth is inversely proportional to the total quality factor Q, the bandwidth of such patch antennas is inherently narrow and can be approximated as [15]

$$BW \approx \frac{1}{Q} = \frac{1}{Q_{rad}} + \frac{1}{Q_{sw}} + \frac{1}{Q_{di}} + \frac{1}{Q_{cu}} \qquad (1)$$

where Q_{sw}, Q_{di} and Q_{cu} account for losses due to surface waves, the dielectric material, and the ohmic losses in the copper (or conductor in general), respectively. For electrically thin and low-loss substrates, the contributions of these loss mechanisms to the bandwidth are small compared to Q_{rad}.

Classical microstrip antenna theory suggests that the bandwidth can be improved by reducing Q_{rad} through an increase in substrate thickness [3]. A thicker dielectric strengthens the fringing fields at the patch edges, leading to stronger radiation and reduced energy storage in the cavity, thereby lowering Q_{rad} and broadening the impedance bandwidth. However, as the height of the patch continues to increase, the setup is better represented by a rectangular plate above a reflector (ground plane), instead of a cavity. Such a rectangular plate is known to offer a wideband dipole mode in terminal antenna applications [16]. On the other hand, numerical analysis using conventional full-wave simulations requires a predefined feed configuration that is well matched to the radiator, complicating efforts to understand how the underlying radiation properties evolve with the patch configuration.

B. Modal Behaviour of a Single-Layer Patch

Given the limitations of the existing theories of patch antennas, CMA enables a more general and explicit investigation of a patch antenna's intrinsic modal behaviour based solely on its geometry and material properties. It decouples the analysis from specific feed types and locations, providing clear insight into the radiation characteristics of all supported modes. Simultaneously, the feed chosen to excite the desired mode(s) can also be included in CMA to analyse and mitigate any negative effect. The feed analysis becomes important in the D band since the feed structure can be electrically large relative to the wavelength.

The nth characteristic mode is associated with the eigenvalue $\lambda_n(f)$, and the corresponding modal significance (MS) is defined as [17]

$$MS_n(f) = \frac{1}{\sqrt{1+\lambda_n^2(f)}}, \quad (2)$$

where $MS_n \in [0, 1]$ and is equal to 1 at resonance when $\lambda_n = 0$. Modes with larger MS_n values indicate higher potential contribution to the use of the structure as a radiator. A mode is generally considered significant when $MS_n \geq 1/\sqrt{2}$, and the contiguous frequency range satisfying this criterion is referred to as the modal bandwidth.

To illustrate the effect of dielectric thickness (or patch height), CMA is applied to a single-layer microstrip patch operating in the D band, modelled using Altair FEKO 2024.1. The configuration consists of an infinite ground plane and an infinitesimally thin rectangular patch, both being perfect electric conductors (see Fig. 1(a)). The HDI PCB substrate used is Panasonic's Megtron 7 5782 ($\varepsilon_r = 3.3$, $\tan\delta = 0.0033$), of variable thickness but with infinite lateral size. In this work, only modes pertaining to the polarisation along the patch's short edge are considered. The modal significance curves for different substrate thicknesses are depicted in Fig. 2, where an increase in thickness can be seen to significantly broaden the modal bandwidth and decrease the resonant frequency.

It is noted that the antenna bandwidth is not identical to the modal bandwidth. The modal bandwidth specifies the frequency range over which a mode has the potential to radiate, whereas the realised antenna bandwidth also depends on the coupling efficiency of the excitation. Therefore, the feed configuration plays a critical role in determining the actual performance.

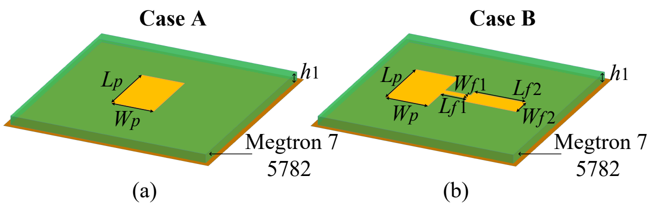

Fig. 1. Configurations of patch models with infinite ground planes. (a) Case A: isolated patch; (b) Case B: same patch fed with a $\lambda/4$ impedance transformer. Dimensions: $L_p = 0.76$ mm, $W_p = 0.49$ mm, $L_{f1} = 0.5$ mm, $L_{f2} = 0.7$ mm, $W_{f1} = 0.05$ mm, $W_{f2} = 0.22$ mm, and $h_1 = 0.1$ mm.

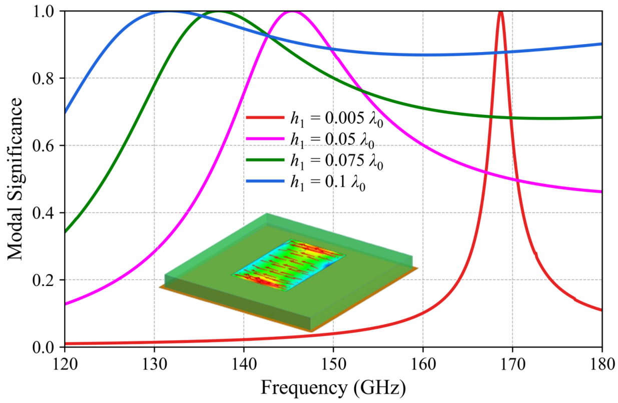

Fig. 2. Modal significance curves of the TM_{10} mode for varying dielectric thicknesses in the isolated patch case (Case A).

Moreover, at lower frequencies such as sub-6 GHz, the feedline can be approximated as electrically short because the length of the conducting trace is often much smaller than λ_0, resulting in negligible current-phase variation. However, in the D band, the length of the narrow conductor can lead to significant current-phase variations. Consequently, the feedline not only delivers power but also acts as a radiator or a parasitic element, potentially creating and exciting additional modes.

To investigate this effect, a quarter-wave ($\lambda/4$) impedance transformer is attached to the isolated patch to match the antenna to a $50\,\Omega$ line, as shown in Fig. 1(b). In the CMA simulation, a microstrip port is connected to the open end of the feedline. The modal significances of the strongly excited modes (with high modal weighting coefficients) are presented in Fig. 3 and compared to that of the isolated patch (Case A). In both cases, the dielectric thickness is fixed at 0.1 mm.

With the feed structure, two co-polarised modes are excited, each exhibiting a narrower modal bandwidth compared to the original TM_{10} mode of the isolated patch, indicated by the dashed red curve. Figure 4 shows the surface-current distributions and normalised electric far-field patterns of the two modes. Mode 1's currents resemble those of the original TM_{10} patch mode, whereas mode 2 has strong currents along three edges of the patch. Therefore mode 2 is a new mode introduced by the feedline, whose boresight radiation pattern slightly differs from that of the TM_{10} mode, as highlighted by

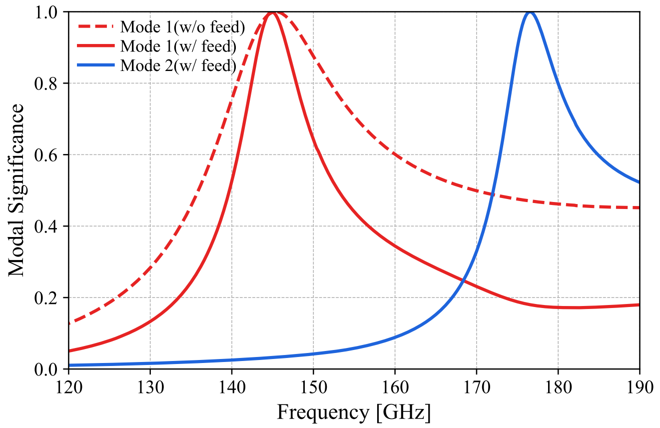

Fig. 3. Modal significance of the excited modes of a patch fed by a $\lambda/4$ impedance transformer.

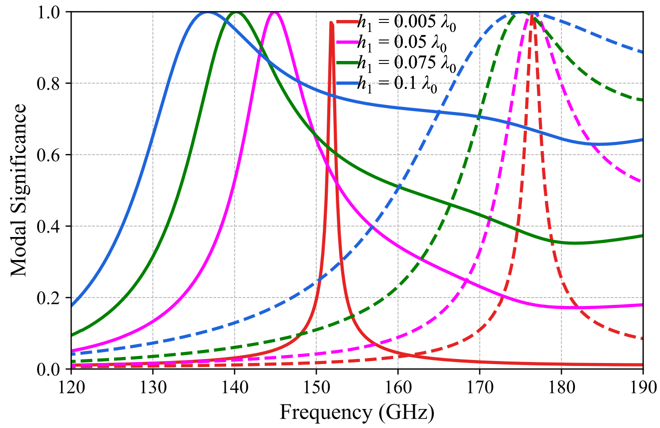

Fig. 5. Modal significances for varying dielectric thickness h_1 in Case B. Modes 1 and 2 are shown in solid and dashed lines, respectively.

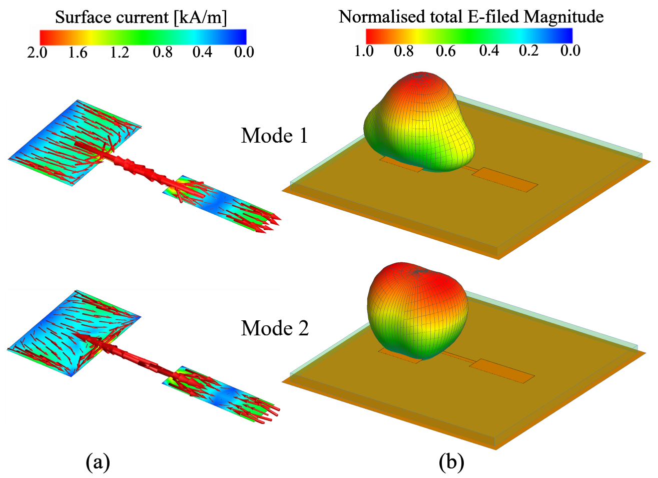

Fig. 4. Surface-current distributions (a) and normalised electric far-field patterns (b) of the excited modes for $h_1 = 0.1$ mm ($0.05\lambda_0$). The far-field patterns are plotted on a linear scale (not in dB) to make the notch clearly visible.

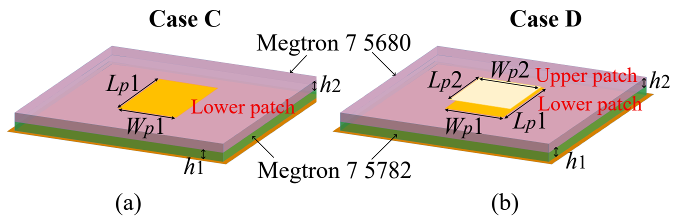

Fig. 6. Configurations of two-layer patch models with infinite ground planes. (a) Case C: dielectric loading; (b) Case D: stacked patches. Dimensions: $L_{p1} = 0.67$ mm, $W_{p1} = 0.44$ mm, $L_{p2} = 0.5$ mm, $W_{p2} = 0.46$ mm, $h_1 = 0.1$ mm, $h_2 = 0.1$ mm.

the linear scale used. Besides, the two resonant frequencies are widely separated, which complicates the merging of these modes to form wideband property. The resonant frequency of mode 2 can be slightly decreased by increasing the patch length L_p, but this measure is insufficient for merging the two resonances. Alternatively, increasing the dielectric thickness can broaden the bandwidth of both modes; however, it also enhances surface waves [15], [18], which increase losses, and further enlarges the separation between the two resonances, as shown in Fig. 5.

C. Modal Behaviour of a Two-Layer Stacked Patch

A single-layer patch with dielectric thickness $h_1 = 0.1$ mm ($0.05\lambda_0$) exhibits a relatively narrow bandwidth and essentially one dominant resonance. Stacked-patch configurations are widely employed to enhance bandwidth, where a parasitic patch of a different size introduces an additional resonance to improve the overall bandwidth. However, suspending a parasitic patch in air is impractical in the D band. Instead, multilayer PCB technologies are used to implement stacked structures, which also introduce dielectric loading and modify the effective permittivity. To examine these effects step by step, Fig. 6 presents two configurations evolved from Case A: Case C only introduces an additional dielectric layer above the patch, whereas Case D implements a stacked patch by adding a second patch above the original patch, separated by the dielectric layer introduced in Case C. In both Cases C and D, the added dielectric layer is Megtron 7 5680 ($\varepsilon_r = 3.06$, $\tan\delta = 0.0029$). The patch dimensions in Cases C and D are first tuned to match the resonant frequency of Case A (to ease comparison), with the lower patch size being kept the same in both configurations.

Figure 7 plots the modal significances of Cases A, C and D. It can be seen that the modal bandwidth of Case A can be enhanced by only adding a dielectric layer, since the increased effective height strengthens the fringing fields and reduces Q_{rad}. In Case D, the parasitic upper patch has a size similar to the lower patch. Specifically, the width W_{p2} of the upper patch is close to W_{p1} of the lower patch, which results in similar resonant frequencies and strong modal coupling. As a result, the modal significance curves merge in the frequency domain, leading to a wider combined modal bandwidth. Moreover, the simulations reveal that increasing the thickness of the upper dielectric layer further increases the bandwidth and decreases

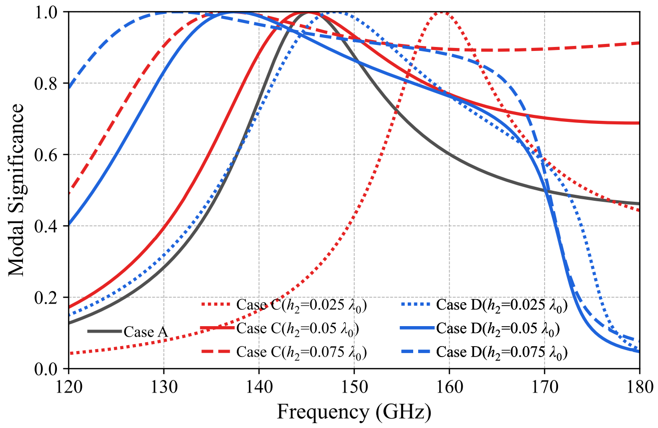

Fig. 7. Modal significances for Cases A, C, and D with varying thicknesses h_2 of the upper dielectric when $h_1 = 0.1$ mm.

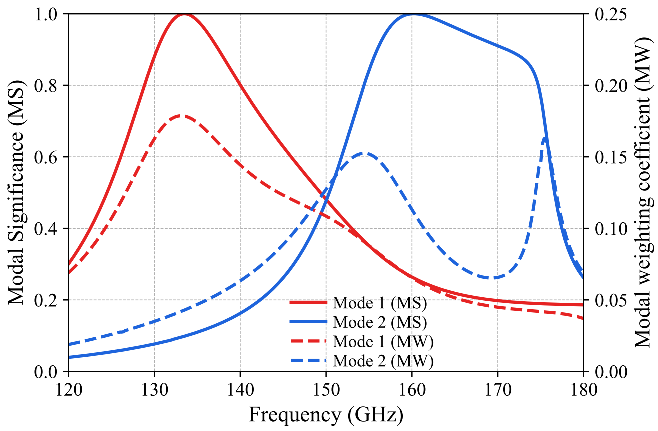

Fig. 8. Modal significance (solid lines) and modal weighting coefficients (dashed lines) of the stacked patch with feedline.

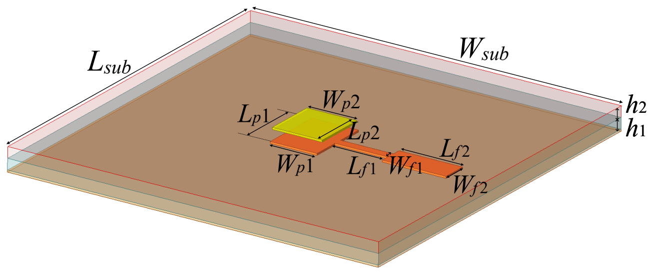

Fig. 9. Geometry and configuration of the final stacked-patch antenna used in full-wave simulation. Dimensions: $L_{p1} = 0.6$ mm, $W_{p1} = 0.45$ mm, $L_{p2} = 0.5$ mm, $W_{p2} = 0.48$ mm, $L_{f1} = 0.5$ mm, $L_{f2} = 0.6$ mm, $W_{f1} = 0.08$ mm, $W_{f2} = 0.195$ mm, $h_1 = 0.1$ mm, $h_2 = 0.1$ mm, $L_{sub} = 4$ mm, $W_{sub} = 4$ mm.

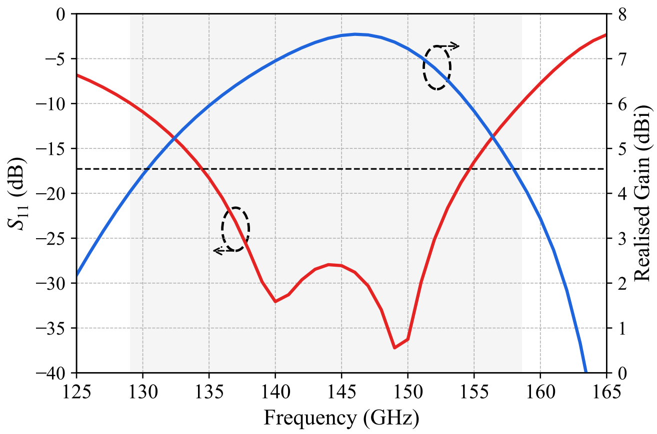

Fig. 10. Simulated $|S_{11}|$ and realised gain of the final practical stacked patch in full-wave simulation. 10 dB impedance bandwidth marked in grey and 3 dB gain bandwidth indicated by intersections with the dashed line.

the resonance frequency.

D. Bandwidth Enhancement of Stacked Patch with Feedline

A parasitic patch can extend the modal bandwidth and thus help to improve the realised bandwidth constrained by the feedline in the single-layer configuration (Case B). Figure 8 presents the modal significances and modal weighting coefficients of a stacked patch antenna with two dielectric layers, fed by a $\lambda/4$ transformer connected to the lower patch and terminated in a 50 Ω microstrip port (i.e., similar to the feed structure of Fig. 1(b)). Each dielectric layer is 0.1 mm ($0.05\lambda_0$) thick. The modal bandwidths of the two excited modes are significantly increased, and the modal weighting coefficient curves exhibit two peaks for each mode. In addition, the introduction of the upper patch also provides additional degrees of freedom to tune the resonances and achieve a wider bandwidth.

III. Full-wave simulation validation

To further validate the broadband performance of the CMA-guided stacked patch antenna design, a more realistic full-wave simulation is carried out in the finite-element method solver of Ansys HFSS 2025 R1. In the simulated model, a finite ground plane and finite dielectric substrates are used, along with 18 µm copper metallisation. The dielectric material thicknesses and properties are unchanged. The antenna dimensions are slightly adjusted to maintain the same resonant frequencies, as shown in Fig. 9.

The simulated results in Fig. 10 demonstrate an impedance bandwidth of 129–158.5 GHz (20.5%), which is slightly wider than the 3 dB gain bandwidth of 130.3–158 GHz (19.2%), with a peak realised gain of 7.54 dBi. Two distinct resonances are observed at 140 GHz and 149 GHz, consistent with the input impedance plot in Fig. 11. Figures 12 and 13 present the corresponding surface-current distributions and normalised radiation patterns at the two frequencies. The properties of the lower resonance (140 GHz) align well with those of Mode 1, whereas the properties of the higher resonance (149 GHz) reflect the combined contributions from Modes 1 and 2, as predicted from the modal weighting results in Fig. 8. Given the close proximity of the two resonances, there is potential to achieve even larger impedance and gain bandwidths, at the cost of reduced peak gain. Moreover, the modal significance and modal weighting coefficient of Mode 2 in Fig. 8 show the potential for even larger bandwidth (to ∼175 GHz). However, this was not achieved due to poor impedance matching of the

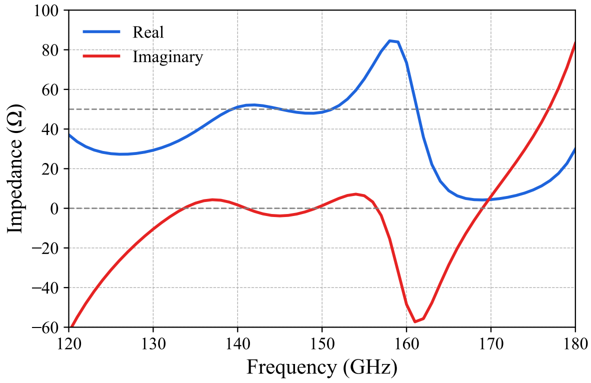

Fig. 11. Real and imaginary parts of the input impedance of the stacked patch in full-wave simulation.

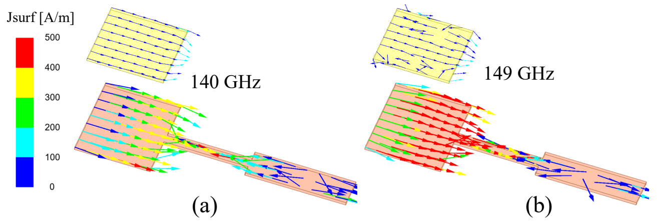

Fig. 12. Simulated surface-current distributions at resonances for the practical stacked patch: (a) 140 GHz; (b) 149 GHz.

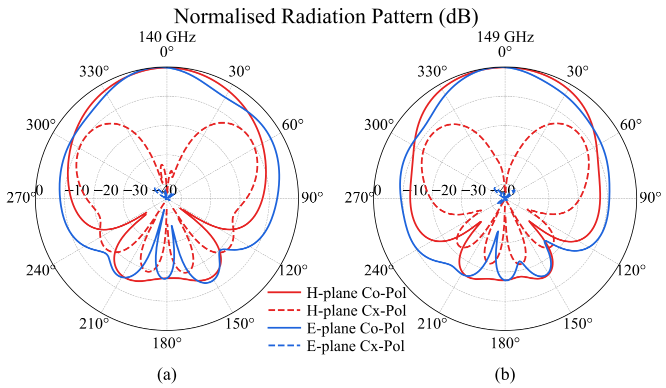

Fig. 13. Simulated normalised E- and H-plane radiation patterns at resonance for the practical stacked patch: (a) 140 GHz; (b) 149 GHz.

adopted feeding structure beyond 160 GHz, as can be observed in Fig. 11. This limitation can be alleviated through further optimization and modification of the feeding structure.

IV. Conclusions

This work revisited the operating principles of single-layer and stacked patch antennas from the perspective of CMA, with a focus on D-band applications. CMA was employed to study the effects of substrate thickness, feed configuration, and stacked topology on modal bandwidth and radiation behaviour. The results show that increasing substrate thickness broadens the modal bandwidth, whereas the feedline reduces it but also introduces a broadside parasitic mode. By adding a stacked parasitic patch, the two modes are broadened, brought closer in frequency and jointly excited, forming a wideband dual-resonance response. Full-wave simulations under realistic conditions confirm the CMA predictions. The final design, implemented in full-wave simulation on a low-cost HDI PCB substrate, achieves an impedance bandwidth of 20.5% and a peak realised gain of 7.54 dBi.

Acknowledgment

This work is supported by the Horizon Europe project 6GTandem.

References

[1] E.-K. Hong, I. Lee, B. Shim, Y.-C. Ko, S.-H. Kim, S. Pack, K. Lee, S. Kim, J.-H. Kim, Y. Shin, Y. Kim, and H. Jung, "6G R&D vision: Requirements and candidate technologies," *J. Commun. Netw.*, vol. 24, no. 2, pp. 232–245, 2022.

[2] H. Kim and J. Oh, "140-GHz wideband array antenna-in-package using multimode resonance," *IEEE Trans. Antennas Propag.*, vol. 71, no. 3, pp. 2136–2144, 2023.

[3] D. Pozar, "Microstrip antennas," *Proc. IEEE*, vol. 80, no. 1, pp. 79–91, 1992.

[4] I. Slomian, I. Piekarz, K. Wincza, and S. Gruszczynski, "Microstrip antenna array with series feeding network designed with the use of slot-coupled three-way power divider," *IEEE Antennas Wireless Propag. Lett.*, vol. 11, pp. 667–670, 2012.

[5] V. S. Jagtap and C. Minot, "Internally integrated active-type patch antenna for semiconductor superlattice THz oscillators," *IEEE Trans. Terahertz Sci. Technol.*, vol. 2, no. 1, pp. 131–136, 2012.

[6] H. Wang, X. B. Huang, and D. G. Fang, "A single layer wideband U-slot microstrip patch antenna array," *IEEE Antennas Wireless Propag. Lett.*, vol. 7, pp. 9–12, 2008.

[7] J.-H. Lee, J. M. Lee, K. C. Hwang, D.-W. Seo, D. Shin, and C. Lee, "Capacitively coupled microstrip comb-line array antennas for millimeter-wave applications," *IEEE Antennas Wireless Propag. Lett.*, vol. 19, no. 8, pp. 1336–1339, 2020.

[8] T. Dao, A. Kearns, D. Reyes Paredes, and G. Hueber, "Wideband high-gain stacked patch antenna array on standard PCB for D-Band 6G communications," *IEEE Antennas Wireless Propag. Lett.*, vol. 23, no. 2, pp. 478–482, 2024.

[9] R. Harrington and J. Mautz, "Theory of characteristic modes for conducting bodies," *IEEE Trans. Antennas and Propag.*, vol. 19, no. 5, pp. 622–628, 1971.

[10] J. J. Adams, S. Genovesi, B. Yang, and E. Antonino-Daviu, "Antenna element design using characteristic mode analysis: Insights and research directions," *IEEE Antennas Propag. Mag.*, vol. 64, no. 2, pp. 32–40, 2022.

[11] M. Khan and D. Chatterjee, "Characteristic mode analysis of a class of empirical design techniques for probe-fed, U-slot microstrip patch antennas," *IEEE Trans. Antennas and Propag.*, vol. 64, no. 7, pp. 2758–2770, 2016.

[12] J. Zeng, X. Liang, L. He, F. Guan, F. H. Lin, and J. Zi, "Single-fed triple-mode wideband circularly polarized microstrip antennas using characteristic mode analysis," *IEEE Trans. Antennas and Propag.*, vol. 70, no. 2, pp. 846–855, 2022.

[13] W.-W. Chen, Q.-S. Wu, and X. Zhang, "Quad-mode dual-band dual-sense circularly polarized microstrip patch antenna," *IEEE Antennas Wireless Propag. Lett.*, vol. 23, no. 5, pp. 1503–1507, 2024.

[14] X. Gao, G. Tian, Z. Shou, and S. Li, "A low-profile broadband circularly polarized patch antenna based on characteristic mode analysis," *IEEE Antennas Wireless Propag. Lett.*, vol. 20, no. 2, pp. 214–218, 2021.

[15] K. Carver and J. Mink, "Microstrip antenna technology," *IEEE Trans. Antennas and Propag.*, vol. 29, no. 1, pp. 2–24, 1981.

[16] H. Li, Y. Tan, B. K. Lau, Z. Ying, and S. He, "Characteristic mode based tradeoff analysis of antenna-chassis interactions for multiple antenna terminals," *IEEE Trans. Antennas Propag.*, vol. 60, no. 2, pp. 490–502, 2012.

[17] J. L. T. Ethier and D. A. McNamara, "Modal significance measure in characteristic mode analysis of radiating structures," *Electron. Letts*, vol. 46, no. 2, pp. 107–108, 2010.

[18] R. Gonzalo, P. De Maagt, and M. Sorolla, "Enhanced patch-antenna performance by suppressing surface waves using photonic-bandgap substrates," *IEEE Trans. Microw. Theory Tech.*, vol. 47, no. 11, pp. 2131–2138, 1999.